ESCUELA DE CONSTRUCCIÓN CIVIL
FACULTAD DE INGENIERÍA
Revista de la Construcción
Journal of Construction

Research Article

Structural behavior of axially loaded high strength concrete columns reinforced longitudinally with glass fibre reinforced polymer bars

Sasikumar P[1], Manju R[2]

[1] Kumaraguru College of Technology, Anna University, Coimbatore (India); sasiserene@gmail.com
[2] Kumaraguru College of Technology, Anna University, Coimbatore (India); manjustructure@gmail.com
*Correspondence: sasiserene@gmail.com

Received: 26.05.2022; **Accepted:** 31.07.2023; **Published:** 31.08.2023

Citation: Sasikumar, P., Manju, R. (2023). Structural behaviour of axially loaded high strength concrete columns reinforced longitudinally with glass fibre reinforced polymer bars. Revista de la Construcción. Journal of Construction, 22(2), 293-305. https://doi.org/10.7764/RDLC.22.2.293.

Abstract: This study investigated the behaviour of axially loaded high strength concrete columns reinforced longitudinally with glass fibre reinforced polymer bars. Total six Reinforced Concrete (RC) columns and six Glass Fibre Reinforced Polymer (GFRP) reinforced concrete columns made with High Strength Concrete (HSC) with the addition of 1.20% of Alkali Resistant Glass Fibre (ARGF). The columns were cast with 1000 mm height and cross-sectional area is 150 mm x 150 mm and were tested under axial loading. The main objective of this study including to increase axial load carrying capacity and stiffness and reduce the ductility, mode of failure, and axial load-displacement response of columns. The RC columns are compared to the GFRP RC columns, and the GFRP RC columns are only carried 90% of the axial load compared to the RC columns. The Finite Element Model (FEM) was used to analyses all columns, and FEM helps predict the axial load.

Keywords: GFRP bar, stiffness, ductility, finite element model, high strength concrete, axial load, displacement.

1. Introduction

Recently reinforced concrete structures have been affected mainly by corrosion due to severe environmental conditions, which affect the strength and durability of concrete structures. Many researchers have conducted corrosion studies to resolve this problem and increase concrete strength. Meanwhile, the construction industry uses high strength concrete, which is better and has more advantages than normal concrete. The high strength concrete is designed to reduce the cross-sectional area of the structural element member. The GFRP is the better solution to replace the traditional reinforcement to overcome corrosion to cast structural elements with high strength concrete using GFRP bars to increase the service life of structural element members. The steel corrosion problems have been studied and solved using new materials (Elchalakani et al., 2020). Fibre reinforced polymers are used in internal reinforcement in several RC structures, including marine construction, bridges, road pavements and deck slab, to be made with high strength concrete (Bouguerra et al., 2011). The high strength concrete circular columns have been studied by many researchers by using FRP bars under axial load (Hadhood et al., 2017b; Hadi et al., 2015; Hales et al., 2016; Hasan et al., 2019; Khorramian & Sadeghian, 2017; Lignola et al., 2011; Mohamed et al., 2014; Pantelides et al., 2013; Samani & Attard, 2012; Vijaya et al., 2020). Some other studies have been conducted under eccentric loading using FRP bars (Fan & Zhang, 2016; Khorramian & Sadeghian, 2017; Salah-Eldin et al., 2019). Only a few researchers have

studied eccentric and concentric loadings conditions (Hadhood et al., 2017a; Hadi et al., 2016; Hadi & Youssef, 2016; Raza & Khan, 2021). The FRP bars square reinforced the RC rectangular and square concrete columns (Ali & El-Salakawy, 2016; Luca, 2010; Tobbi et al., 2012). Based on several researchers has been studied concrete columns of normal strength on concrete, but only limited studies have been done with high strength concrete (Hadhood et al., 2017b; Hales et al., 2016).

2. Materials and methods

2.1. *High strength concrete*

The High Strength Concrete (HSC) columns were designed with M_{70} grade of concrete according to Indian standard 10262-2019. A total of 12 columns were made with HSC, with and without the addition of 1.20% ARGF; all columns were tested after 28 days of curing periods.

2.2. *Steel and GFRP bars*

The 12mm deformed steel and ribbed GFRP bar were made with high strength concrete. The deformed and ribbed bars are shown in Fig.1 and represent the mechanical properties of steel and GFRP bars in Table 1. The 12mm bar was used longitudinally, and the 8 mm bar was used in lateral directions in columns.

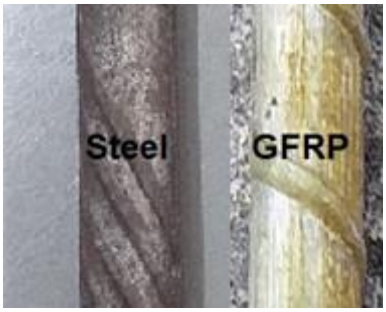

Figure 1. Steel and GFRP bar.

Table 1. Mechanical properties of steel and GFRP bars.

Specimen	Bar dia (mm)	Grade	Stress (MPa)	Young's modulus (GPa)
Steel	12	500	463	200
GFRP	12	890	863	38

2.3. *Design of column*

Steel and GFRP RC columns were designed with the following two equations: axial load capacity is evaluated based on the concrete strength and the columns cross-section area. The role of the GFRP bars does not find in (CAS 2012) and (ACI 440, 2015). Based on the previous literature study, the GFRP bars are mainly considered to carry the axial load on the columns. (Hadi et al., 2016; Maranan et al., 2016; Tobbi et al., 2012). It's tough to determine the axial load carrying capacity on concrete columns using GFRP bars due to the different modes of failure in columns. The axial load is determined using Eq. (1) (Afifi et al., 2014). According to the test results, the axial load of 60% was only carried out compared to Eq. (1), But Eq. (2) gave a better correlation comparison of experimental load is presented in Table 2. The concrete area contributed around 0.85 of the compressive strength (ACI 2008).

$$P_n = 0.85 \times f_c \times (A_g - A_{FRP}) + 0.35 \times f_{u\,FRP} \times A_{FRP} \quad (1)$$

$$P_P = A_c P_{ck} + A_s P_{sk} \quad (2)$$

where:
$P_{ck} = 0.4\,(f_{ck})$ and
$P_{sk} = 0.67 f_y$

A_c and A_g represented the area of concrete; A_s represented the area of longitudinal reinforcement; P_{ck} and f_c denoted compressive strength of concrete; P_{sk} denoted yield strength of longitudinal support; A_{FRP} which means the cross-sectional area of the GFRP longitudinal reinforcement; $f_{u\ FRP}$ represented the ultimate tensile strength of the GFRP bar.

Table 2. Comparison of axial loads with various questions

Specimen ID	Experimental load (kN)	Eq. (1)	Eq. (2)
RCC-1	986	0.65	1.15
RCC-2	994	0.66	1.16
RCC-3	982	0.65	1.15
RCC-F-1	1072	0.67	1.20
RCC-F-2	1081	0.68	1.21
RCC-F-3	1087	0.68	1.21
GFRP-1	886	0.58	0.92
GFRP-2	875	0.57	0.90
GFRP-3	882	0.58	0.91
GFRP-F-1	967	0.60	0.96
GFRP-F-2	973	0.61	0.97
GFRP-F-3	978	0.61	0.97

Note - RCC: Reinforced cement concrete columns: RCC-F: Reinforced cement concrete columns with 1.20% of ARGF; GFRP – Glass Fibre Reinforced concrete columns; GFRP-F: Glass Fibre Reinforced concrete columns with 1.20% of ARGF

2.4. *Specimen preparation and loading setup*

Twelve columns were cast (six steel and six GFRP RC columns); the details are summarised in Table 3. Steel and GFRP RC cage were prepared and placed on the steel mould, and the reinforcement details were represented in Fig. 2. The high strength concrete was poured on the steel mould and compacted using the tamping rod; finally, the concrete was levelled using a trowel. The high strength concrete columns were removed from the steel mould without any damage and cured for 28 days. All columns were tested after a curing period of 28 days. All column specimens were tested under the loading frame capable of 200 T, as shown in Fig. 3. The columns were placed on the loading frame, and the column was aligned centre. Both ends are considered hinged support conditions, and 10mm thick steel plates are placed at the bottom and top columns. Totally linear variable differential transformers were used, two were placed in the lateral direction, and one was placed in the vertical direction to measure the vertical displacement.

Table 3. Specimen details of columns

Specimen ID	Specimen dimensions (mm)			Longitudinal reinforcement	Transverse reinforcement
	B	D	L		
RCC-1	150	150	1000	4 Nos. #12mm	#8mm @ 80mm c/c
RCC-2					
RCC-3					
RCC-F-1					
RCC-F-2					
RCC-F-3					
GFRP-1					
GFRP-2					
GFRP-3					
GFRP-F-1					
GFRP-F-2					
GFRP-F-3					

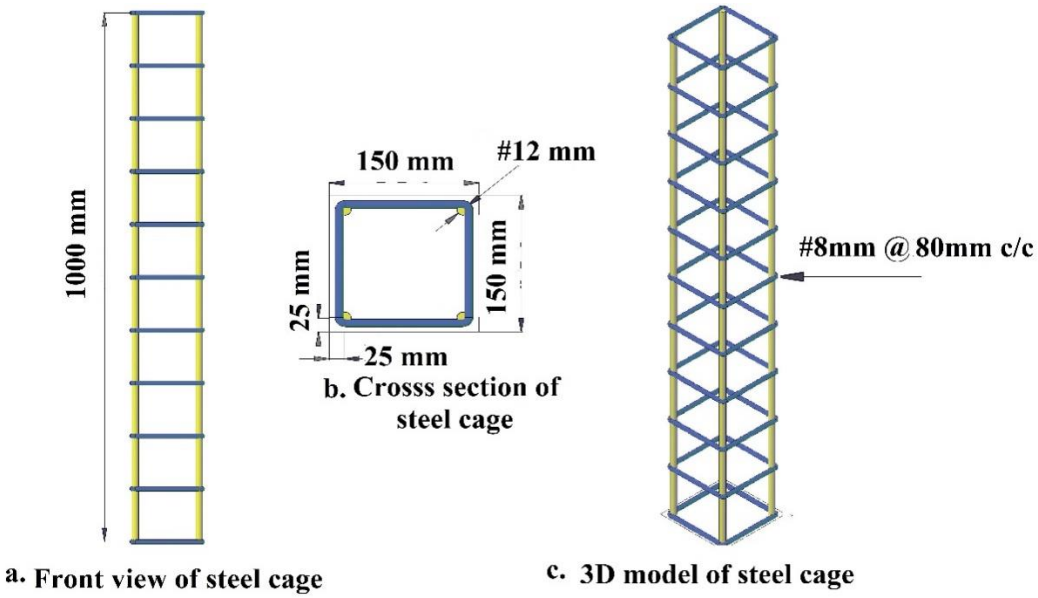

Figure 2. Geometry properties of columns.

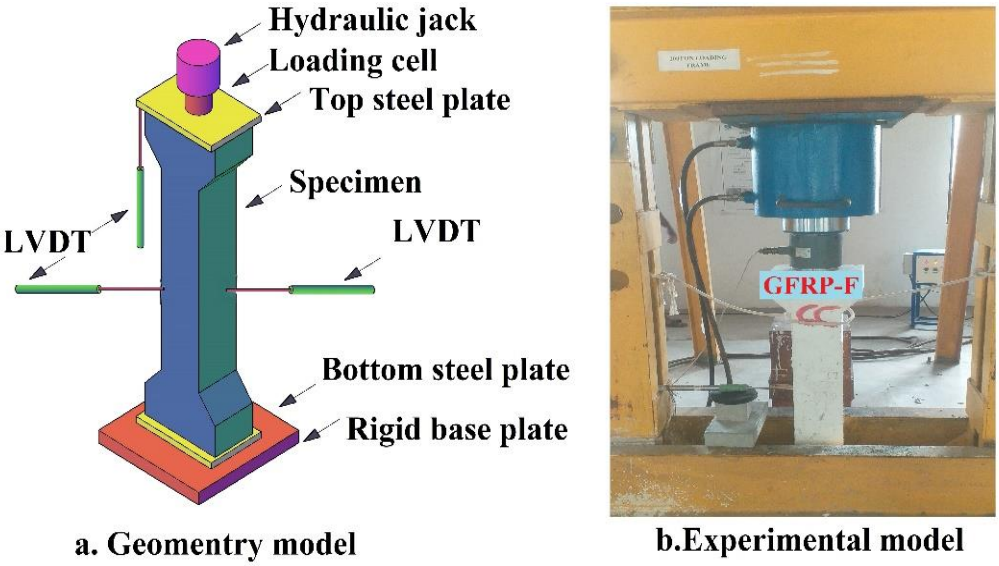

Figure 3. Column setup for testing.

3. Analytical study

3.1. Modelling and mesh of columns

The RCC and GFRP RC columns are modelled using ANSYS software, as shown in Fig. 4. The columns are considered as two parts (plain cement concrete and high strength reinforcement cage). Totally three types of mesh were used to analyses the columns (Coarse, medium and fine); the coarse mesh gave a better prediction of the axial load of columns is presented in Fig. 5.

Figure 4. 3D modelling of high strength concrete column.

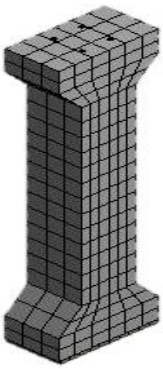

Figure 5. Mesh of high strength concrete column.

3.2. Support condition

The end condition of the column specimen is considered as both ends hinged, Fig. 6 represented in the boundary condition of the column. The maximum axial displacement of columns is the top portion of the column.

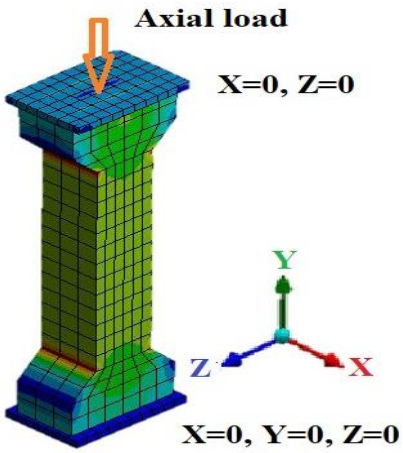

Figure 6. Loading condition of the column.

4. Results and discussion

4.1. Comparison between experimental and analytical results

The high strength concrete columns are considered the two groups, and each group have six columns (RCC-1, RCC-2, RCC-3, RCC-F-1, RCC-F-2, RCC-F-3, GFRP-1, GFRP-2, GFRP-3, GFRP-F-1, GFRP-F-2, GFRP-F-3). Each group of columns have cast with and without ARGF. RCC-F and GFRP-F columns have high axial load carrying capacity compared to the RCC and GFRP columns are summarized in Table 4. The design axial loads are compared with the experimental axial load, and the experimental axial load is compared with the analytical axial load is presented in Table 5. The axial load carrying capacity of the GFRP and GFRP-F columns have taken only 90% compared to the RCC and RCC-F columns. The experimental and analytical axial displacement of all columns were displayed in Figs. 7 & 8.

Table 4. Comparison between experimental and analytical loads.

ID	Experimental load (kN)	Stress (N/mm^2)	Avge stress (N/mm^2)	Analytical load (kN)	Stress (N/mm^2)	Avge stress (N/mm^2)
RCC-1	986	43.82	43.88	990	44.00	44.06
RCC-2	994	44.18		998	44.36	
RCC-3	982	43.64		986	43.82	
RCC-F-1	1072	47.64	48.00	1080	48.00	48.30
RCC-F-2	1081	48.04		1088	48.36	
RCC-F-3	1087	48.31		1092	48.53	
GFRP-1	886	39.38	39.16	892	39.64	39.35
GFRP-2	875	38.89		878	39.02	
GFRP-3	882	39.20		886	39.38	
GFRP-F-1	967	42.98	43.23	974	43.29	43.50
GFRP-F-2	973	43.24		978	43.47	
GFRP-F-3	978	43.47		984	43.73	

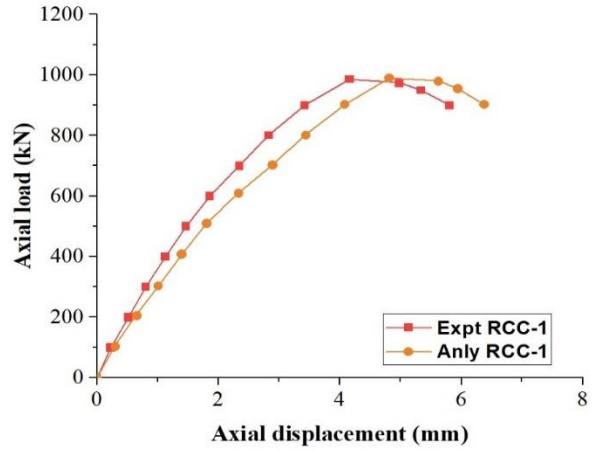

a. RCC-1

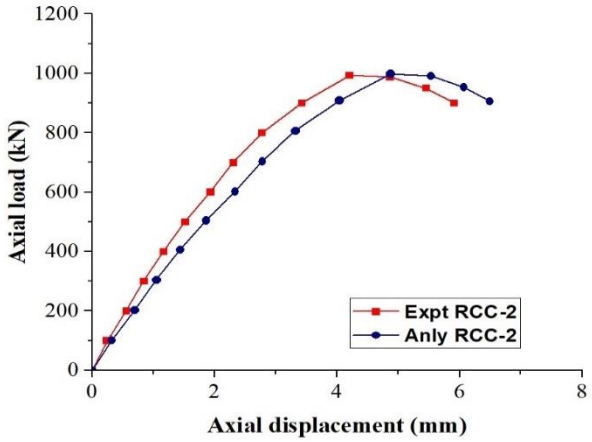

b. RCC-2

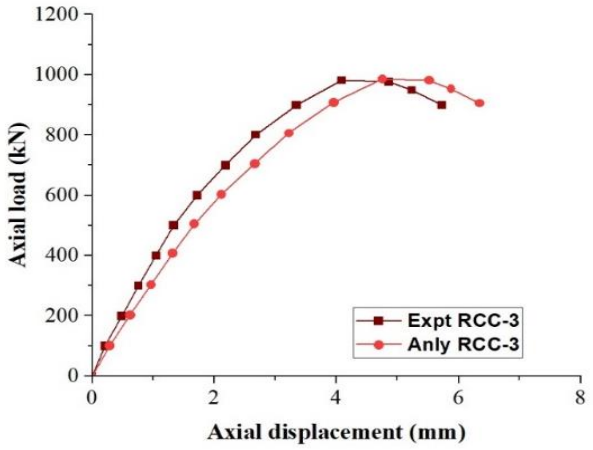

c. RCC-3

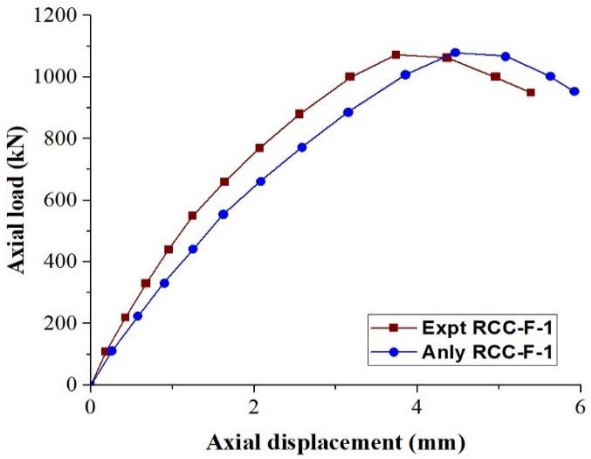

d. RCC-F-1

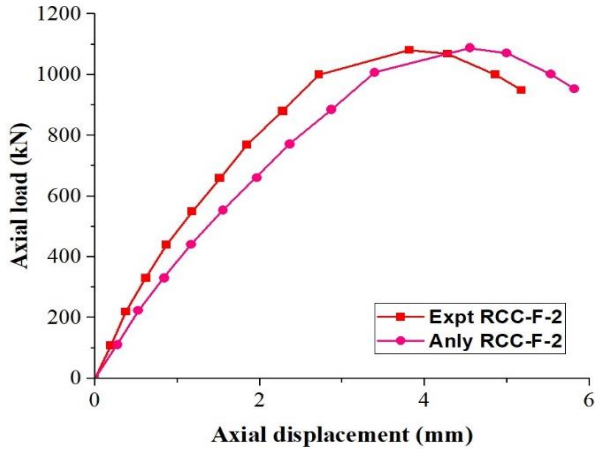

e. RCC-F-2

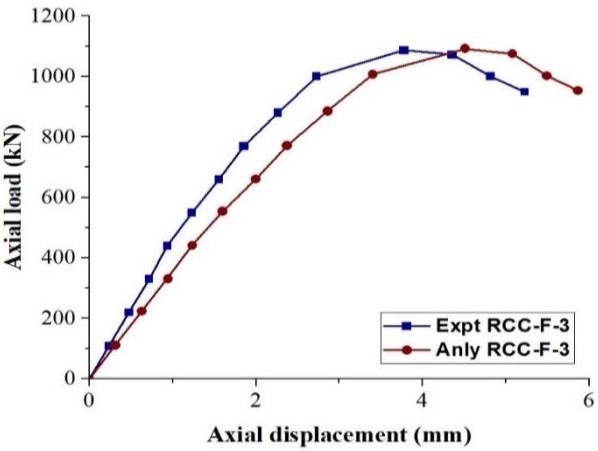

f. RCC-F-3

Figure 7. Axial load Vs Axial displacement responses for RC columns.

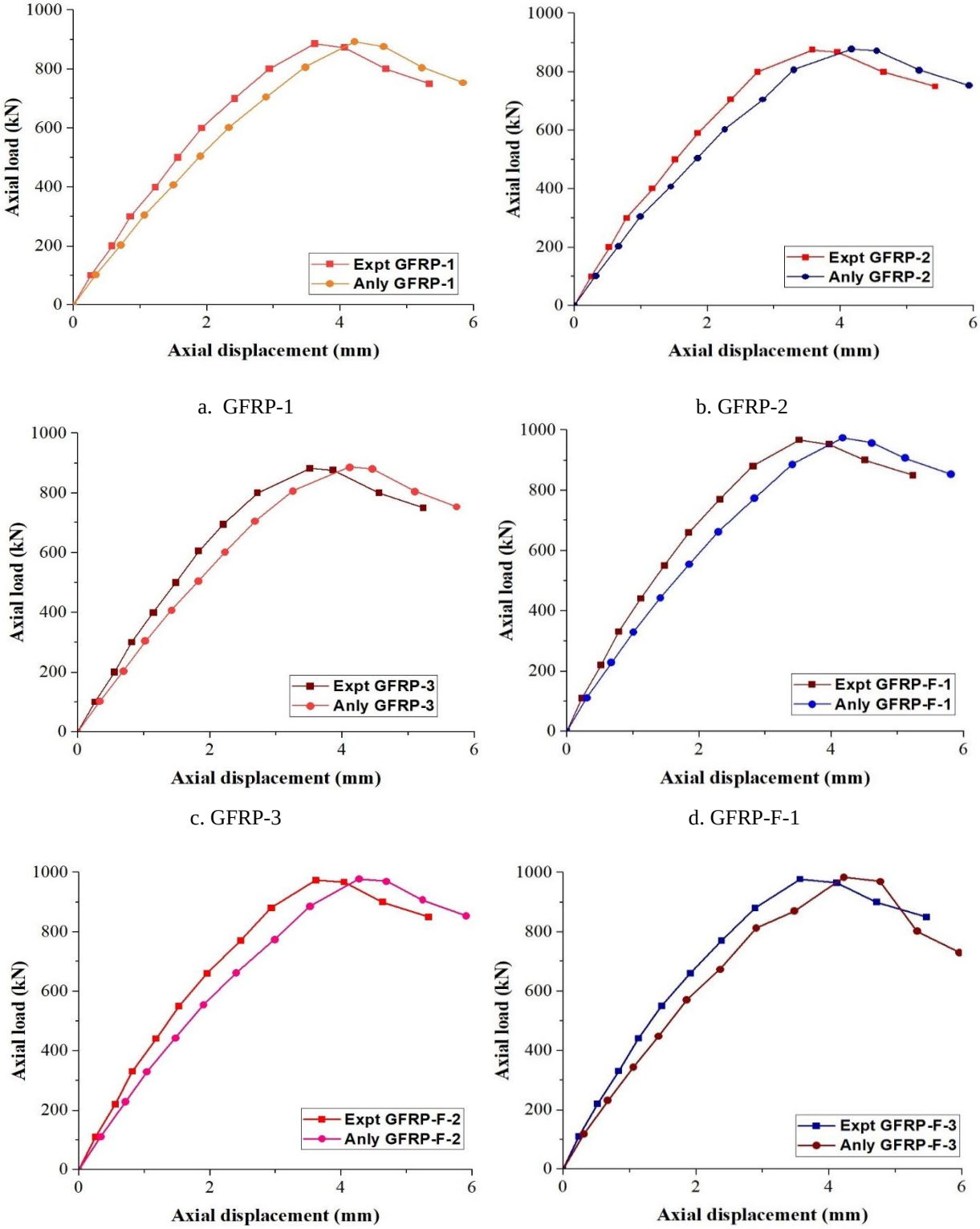

a. GFRP-1 b. GFRP-2

c. GFRP-3 d. GFRP-F-1

e. GFRP-F-2 f. GFRP-F-3

Figure 8. Axial load Vs Axial displacement responses for GFRP RC columns.

Table 5. Comparison between design, experimental and analytical loads.

ID	Design load (kN)	Experimental load (kN)	Analytical load (kN)	P_{anly} / P_{expt}	P_{expt} / P_{design}
RCC-1	855	986	990	1.16	1.15
RCC-2	855	994	998	1.17	1.16
RCC-3	855	982	986	1.15	1.15
RCC-F-1	895	1072	1080	1.21	1.20
RCC-F-2	895	1081	1088	1.22	1.21
RCC-F-3	895	1087	1092	1.22	1.21
GFRP-1	968	886	892	0.92	0.92
GFRP-2	968	875	878	0.91	0.90
GFRP-3	968	882	886	0.92	0.91
GFRP-F-1	1007	967	974	0.97	0.96
GFRP-F-2	1007	973	978	0.97	0.97
GFRP-F-3	1007	978	984	0.98	0.97
Mean		-	-	1.07	1.06
Standard deviation		-	-	0.13	0.13
Coefficient of variation		-	-	12.27	12.27

4.2. Failure mode of all columns

Table 6 reported the different modes of failure in all columns. Based on the experimental study, the common observation from all columns has a concrete crushing failure. Some columns have concrete splitting, concrete cover spalling, and fibre pull out failure. The hairline crack is formed when the columns have reached the yield point, the axial load is gradually increased up to the ultimate load, and the cracks also develop. After getting the ultimate load, the columns reached the failure; the ultimate and failure load are represented in Table 6. RCC columns failed with wide cracks when they went through the ultimate load; the concrete cover spalling and concrete splitting were presented after the failure of column specimens. The axial displacement was gradually increased during the period of testing. The same as RCC-F columns failed with concrete crushing and fibre pull out during the test period. The failure modes in RCC, RCC-F, GFRP and GFRP-F columns are similar but axial, only varying compared to both groups.

Table 6. Mode of failure of all columns.

ID	Ultimate load (kN)		Failure load (kN)		Mode of failure
	Expt	Anly	Expt	Anly	
RCC-1	986	990	974	981	CS + CC + CCS
RCC-2	994	998	987	992	CS + CC
RCC-3	982	986	978	982	CC + CCS
RCC-F-1	1072	1080	1063	1067	CC + FP
RCC-F-2	1081	1088	1068	1072	CC
RCC-F-3	1087	1092	1072	1076	CC + FP
GFRP-1	886	892	873	876	CC
GFRP-2	875	878	868	872	CC + CS
GFRP-3	882	886	876	880	CC + CS + CCS
GFRP-F-1	967	974	953	957	CC
GFRP-F-2	973	978	967	970	CC + FP
GFRP-F-3	978	984	965	972	CC + FP

Note - CC: Concrete crushing; FP: Fibre pull out; CS: Concrete Splitting; CCS: Concrete Cover Spalling

Figure 9. Mode of failure in all columns.

4.3. Ductility index

According to the experimental study, the columns are considered in three phases as shown in Fig.10. The first phase has no cracks in the elastic limit. In the second phase, the column gradually went from elastic to plastic limit simultaneously the hairline cracks also formed in columns; the non-linear behaviour was observed from this stage (Δ_y). The concrete cover spalling was obtained from the columns when the maximum axial load reached the concrete and longitudinal reinforcement (Δ_u). In this third stage, the columns area was reduced effectively and concrete cover spalling occurred partially or entirely. The columns have more durable before reaching the plastic stage. Based on the experimental test results, the ductility and stiffness are summarised in Table 7, and experimental and analytical results are also compared. The ductility index μ_Δ was calculated by Eq. (3); the ductility index is defined as the ratio between the ultimate displacement to yield displacement and ductility index is represented in Fig.11.

$$\text{Ductility index } \mu_\Delta = \frac{\Delta u}{\Delta y} \tag{3}$$

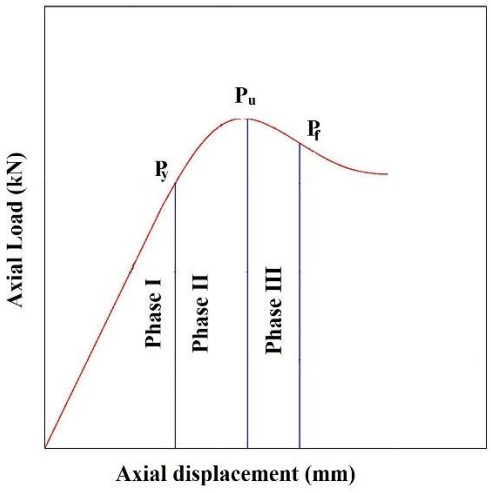

Figure 10. Axial load Vs displacement curve.

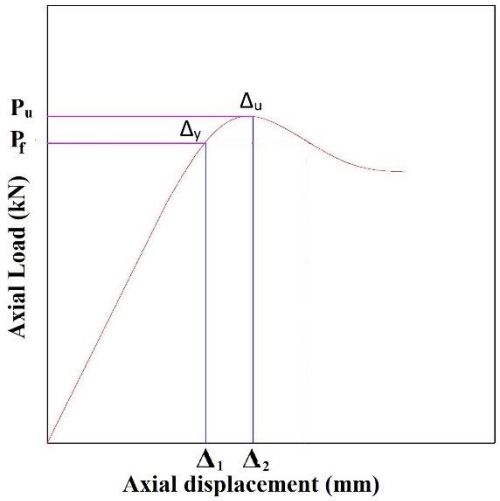

Figure 11. Ductility index.

Table 7. Comparison between experimental and analytical ductility and stiffness.

ID	Yield point		Ultimate point		Ductility factor (μ_Δ)	Stiffness (k) (kN/mm)
	P_y (kN)	D_y (mm)	P_u (kN)	D_u (mm)		
RCC-1	705	2.35	986	4.16	1.77	237.02
RCC-2	712	2.31	994	4.21	1.82	236.10
RCC-3	707	2.19	982	4.09	1.87	240.10
RCC-F-1	773	2.56	1072	3.74	1.46	286.63
RCC-F-2	779	2.48	1081	3.82	1.54	282.98
RCC-F-3	768	2.52	1087	3.78	1.50	287.57
GFRP-1	694	2.42	886	3.62	1.50	244.75
GFRP-2	702	2.36	875	3.58	1.52	244.41
GFRP-3	698	2.21	882	3.52	1.59	250.57
GFRP-F-1	758	2.41	967	3.52	1.46	274.72
GFRP-F-2	763	2.47	973	3.62	1.47	268.78
GFRP-F-3	756	2.39	978	3.57	1.49	273.95

5. Conclusion

The present study was carried out the high strength concrete columns using steel and GRFP bars under axial loading. Based on the experimental and analytical results, the following conclusions are summarised.

1. According to the experimental test results of GFRP, the reinforced concrete columns performed similarly to the steel reinforced concrete columns. The addition of alkaline resistant glass fibre on steel and GFRP reinforced concrete columns increased axial load carrying capacity compared to the without alkaline resistant glass fibre on steel, and GFRP reinforced concrete columns.
2. Steel and GFRP RC columns failed in concrete crushing after reaching the ultimate load. Meanwhile, steel RC columns failed near the support and had minor cracks, but GFRP RC columns failed with wide cracks.
3. The axial load was increased constantly up to the ultimate load; after the failure of columns, the axial load decreased. The steel RC columns axial load is increased uniformly, but some GFRP RC columns failed suddenly after reaching the ultimate load. Steel and GFRP RC columns axial load-displacement were performed similarly.
4. The axial load carrying capacity of the RCC-F and GFRP-F RC columns is higher compared to the RCC and GFRP RC columns. The GFRP and GFRP-F RC columns carried only 90% of the axial load compared to the RCC and RCC-F RC columns.
5. All column's axial load strengths were compared with two equations. The experimental results were compared with both equations; equation two was given a better correlation than equation one.
6. Ductility and stiffness are more critical in RCC structures; when fibre add to RCC-F and GFRP-F RC columns, the ductility is reduced, and stiffness is increased; meanwhile, in RCC and GFRP RC columns, the ductility is improved, and stiffness is decreased.
7. According to the test results, the GFRP bars are suitable for steel reinforcement in severe environmental conditions.
8. The FEM analysis and experimental axial load-displacement curve showed a better correlation. The FEM analysis helped predict the experimental results; the analytical results were compared with the experimental results.

Author contributions: Sasikumar P: Participation in planning for the study, design, analytical, experimental parametric study, research methodology, implementation of the parametric study, and writing original manuscript preparation. Manju R: Review and enhance the paper manuscript, supervising experimental works.

Funding: No funding agency has supported this project.

Acknowledgements: The authors gratefully acknowledge the Kumaraguru College of Technology for providing all the required facilities to accomplish this study.

Conflicts of interest: The authors declare no conflicts of interest.

References

ACI 318-08 (2008). Building code requirements for structural concrete and commentary.

ACI 440.1R-03 (2015). Guide for the design and construction of concrete reinforced with FRP bars. In American Concrete Institute (ACI), Farmington Hills, Mich., USA (p. 42pp).

Afifi, M. Z., Mohamed, H. M., & Benmokrane, B. (2014). Axial Capacity of Circular Concrete Columns Reinforced with GFRP Bars and Spirals. Journal of Composites for Construction, 18(1), 04013017.

AlAjarmeh, O. S., Manalo, A. C., Benmokrane, B., Karunasena, W., Mendis, P., & Nguyen, K. T. Q. (2019). Compressive behavior of axially loaded circular hollow concrete columns reinforced with GFRP bars and spirals. Construction and Building Materials, 194, 12–23. https://doi.org/10.1016/j.conbuildmat.2018.11.016

Ali, M. A., & El-Salakawy, E. (2016). Seismic Performance of GFRP-Reinforced Concrete Rectangular Columns. Journal of Composites for Construction, 20(3), 04015074.

Bouguerra, K., Ahmed, E. A., El-Gamal, S., & Benmokrane, B. (2011). Testing of full-scale concrete bridge deck slabs reinforced with fiber-reinforced polymer (FRP) bars. Construction and Building Materials, 25(10), 3956–3965.

CSA (2012). Design, and construction of building structures with fibre-reinforced polymers.

Elchalakani, M., Dong, M., Karrech, A., Mohamed Ali, M. S., & Huo, J. S. (2020). Circular Concrete Columns and Beams Reinforced with GFRP Bars and Spirals under Axial, Eccentric, and Flexural Loading. Journal of Composites for Construction, 24(3), 04020008.

Fan, X., & Zhang, M. (2016). Behaviour of inorganic polymer concrete columns reinforced with basalt FRP bars under eccentric compression: An experimental study. Composites Part B: Engineering, 104, 44–56.

Hadhood, A., Mohamed, H. M., & Benmokrane, B. (2017a). Experimental Study of Circular High-Strength Concrete Columns Reinforced with GFRP Bars and Spirals under Concentric and Eccentric Loading. Journal of Composites for Construction, 21(2), 04016078.

Hadhood, A., Mohamed, H. M., & Benmokrane, B. (2017b). Strength of circular HSC columns reinforced internally with carbon-fiber-reinforced polymer bars under axial and eccentric loads. Construction and Building Materials, 141, 366–378.

Hadi, M. N. S., Karim, H., & Sheikh, M. N. (2016). Experimental Investigations on Circular Concrete Columns Reinforced with GFRP Bars and Helices under Different Loading Conditions. Journal of Composites for Construction, 20(4), 04016009.

Hadi, M. N. S., Wang, W., & Sheikh, M. N. (2015). Axial compressive behaviour of GFRP tube reinforced concrete columns. Construction and Building Materials, 81, 198–207.

Hadi, M. N. S., & Youssef, J. (2016). Experimental Investigation of GFRP-Reinforced and GFRP-Encased Square Concrete Specimens under Axial and Eccentric Load and Four-Point Bending Test. Journal of Composites for Construction, 20(5), 04016020.

Hales, T. A., Pantelides, C. P., & Reaveley, L. D. (2016). Experimental Evaluation of Slender High-Strength Concrete Columns with GFRP and Hybrid Reinforcement. Journal of Composites for Construction, 20(6), 04016050.

Hasan, H. A., Sheikh, M. N., & Hadi, M. N. S. (2019). Maximum axial load carrying capacity of Fibre Reinforced-Polymer (FRP) bar reinforced concrete columns under axial compression. Structures, 19, 227–233.

Karim, H., Sheikh, M. N., & Hadi, M. N. S. (2016). Axial load-axial deformation behaviour of circular concrete columns reinforced with GFRP bars and helices. Construction and Building Materials, 112, 1147–1157.

Khorramian, K., & Sadeghian, P. (2017). Experimental and analytical behavior of short concrete columns reinforced with GFRP bars under eccentric loading. Engineering Structures, 151, 761–773.

Luca, D. A., Matta, F., Nanni, A. (2010). Behavior of full-scale GFRP reinforced concrete columns under axial load. ACI Structural Journal 105,1-31.

Maranan, G. B., Manalo, A. C., Benmokrane, B., Karunasena, W., & Mendis, P. (2016). Behavior of concentrically loaded geopolymer-concrete circular columns reinforced longitudinally and transversely with GFRP bars. Engineering Structures, 117, 422–436. https://doi.org/10.1016/j.engstruct.2016.03.036

Mohamed, H. M., Afifi, M. Z., & Benmokrane, B. (2014). Performance Evaluation of Concrete Columns Reinforced Longitudinally with FRP Bars and Confined with FRP Hoops and Spirals under Axial Load—Journal of Bridge Engineering, 19(7), 04014020.

Pantelides, C. P., Gibbons, M. E., & Reaveley, L. D. (2013). Axial Load Behavior of Concrete Columns Confined with GFRP Spirals. Journal of Composites for Construction, 17(3), 305–313.

Raza, A., & Khan, Q. uz Z. (2021). Structural Behavior of GFRP-Reinforced Circular HFRC Columns Under Concentric and Eccentric Loading. Arabian Journal for Science and Engineering, 46(5), 4239–4252.

Salah-Eldin, A., Mohamed, H. M., & Benmokrane, B. (2019). Structural performance of high-strength-concrete columns reinforced with GFRP bars and ties subjected to eccentric loads. Engineering Structures, 185(November 2018), 286–300.

Samani, A. K., & Attard, M. M. (2012). A stress-strain model for uniaxial and confined concrete under compression. Engineering Structures, 41, 335–349.

Tobbi, H., Farghaly, A. S., & Benmokrane, B. (2012). Concrete columns reinforced longitudinally and transversally with glass fiber-reinforced polymer bars. ACI Structural Journal, 109(4), 551–558.

Vijaya, B., Selvan, S. S., & Vasanthi, P. (2020). Experimental investigation on the behaviour of reinforced concrete column containing manufactured sand under axial compression. Materials Today: Proceedings, 39, 446–453.